Japanese Journal of Applied Physics
Vol. 45, No. 5B, 2006, pp. 4706–4711

Generation of Strain Inside Objects Using Dual Acoustic Radiation Force

Hideyuki HASEGAWA, Mikito TAKAHASHI, Yoshifumi NISHIO and Hiroshi KANAI*

Graduate School of Engineering, Tohoku University, Sendai 980-8579, Japan

(Received November 30, 2005; accepted February 15, 2006; published online May 25, 2006)

Many studies have been carried out on the measurement of mechanical properties of tissues by applying an acoustic radiation force induced by ultrasound to an object. However, one acoustic radiation force in a given direction (e.g., vertical direction) does not generate strain in an object effectively because it also causes changes in the object's position, which has zero spatial gradient in displacement (= no strain). Especially when the elastic modulus of the object is much higher than that of the surrounding tissue (such as a tumor in breast tissue), one acoustic radiation force might generate only a change in the position of the object unlike a strain in the object is hardly generated. In such cases, mechanical properties of the object cannot be evaluated. In this study, two cyclic acoustic radiation forces are simultaneously applied to an object in two different directions (e.g., two opposite horizontal directions) to effectively generate strain inside the object, even when the object is much harder than the surrounding tissue. [DOI: 10.1143/JJAP.45.4706]

KEYWORDS: dual acoustic radiation force, strain, mechanical property

1. Introduction

In recent years, some remote actuation methods based on acoustic radiation force have been reported. Fatemi and coworkers proposed an imaging method called ultrasound-stimulated acoustic emission (USAE).[1,2] Their system consists of two confocal ultrasonic transducers, and two ultrasound beams with two slightly different frequencies, f and $(f + \Delta f)$, are transmitted. Acoustic radiation pressure, $P_R(t)$, exerted on the interface between two different media is a function of the energy density, $e(t)$, and the specific acoustic impedances, Z_1 and Z_2, of the media.[3] The energy density, $e(t)$, is proportional to the square of the sum of the sound pressures, $p_1(t)$ and $p_2(t)$, generated by the two transducers. In the intersectional area of these two beams, therefore, an oscillatory radiation pressure $P_R(t)$ at the frequency difference, Δf, is applied to the interface. The radiation force produces acoustic emission which is closely related to the mechanical frequency response of the medium. By measuring the acoustic emission with a hydrophone, hard inclusions in soft material may be experimentally detected. The spatial resolution in the depth direction corresponds to the size of the intersectional area.

Nightingale *et al.* proposed an alternative imaging method in which pulsed ultrasound is employed to apply the radiation force to a soft tissue during short durations (less than 1 ms). The viscoelastic properties of the tissue are measured from the magnitude and the transient response of the displacement, $d(t)$, of the tissue.[4–6] In order to generate measurable displacement, $d(t)$, by several ultrasonic pulses, high-intensity pulsed ultrasound of $1{,}000\,W/cm^2$ is employed. According to the safety guidelines provided by the Japan Society of Ultrasonics in Medicine (JSUM), however, the intensity of ultrasound is recommended to be less than $240\,mW/cm^2$ and $1\,W/cm^2$ for pulsed and continuous waves, respectively.[7] Therefore, the intensity of the pulsed ultrasound employed by Nightingale *et al.* is far greater than that indicated in the safety guidelines.

To improve the spatial resolution in measurements of the response of an object, Michishita *et al.* used an ultrasound correlation-based method, the ultrasonic *phased tracking method*,[8,9] to measure the minute displacement, $d(t)$, caused by the acoustic radiation force.[10] The accuracy in the displacement measurement by the *phased tracking method* was evaluated to be 0.2 μm by basic experiments using a rubber plate,[11] and influences of the focal position of the ultrasonic beam and the change in center frequency of RF echo due to the frequency-dependent attenuation in tissue on the measurement accuracy were also investigated.[12–14] Furthermore, the *phased tracking method* was modified to be more robust against noise[15] and to have a better spatial resolution.[16] The *phased tracking method* has been already applied to measurements of spontaneous or externally applied vibrations and viscoelasticity of the arterial wall[17–26] and heart wall.[27–33]

In addition, to suppress the sound pressure of the ultrasound employed, a CW ultrasound, which consists of the sum of the frequency components at f and $f + \Delta f$, was employed to cyclically actuate the acoustic radiation pressure, $P_R(t)$, at a low frequency Δf to increase the signal-to-noise ratio in the estimated displacement.[10]

However, one acoustic radiation force in a given direction (e.g., vertical direction) does not generate strain in an object effectively because it also causes a change in the object's position, which has zero spatial gradient in displacement (= no strain). Especially when the elastic modulus of the object is far greater than that of the surrounding media, one acoustic radiation force may generate only a change in the position of the object as illustrated in Fig. 1(a). In such cases, the mechanical properties of the object cannot be estimated. In this study, for effective generation of strain inside the object even in such cases, two acoustic radiation forces with phases of ϕ and $\phi + \Delta\phi$ were applied to two different positions in the object from two different directions (e.g., two opposite horizontal directions) as shown in Fig. 1(b). The displacements of the region inside the object, where the two acoustic radiation forces were applied, were measured by the ultrasonic *phased tracking method.*

2. Principles

When a continuous plane-wave ultrasound is incident on an interface between two different media, a constant force, which is called an acoustic radiation force, is exerted on the interface. Acoustic radiation pressure, $P_R(t)$, is defined as the

*E-mail address: hasegawa@us.ecei.tohoku.ac.jp

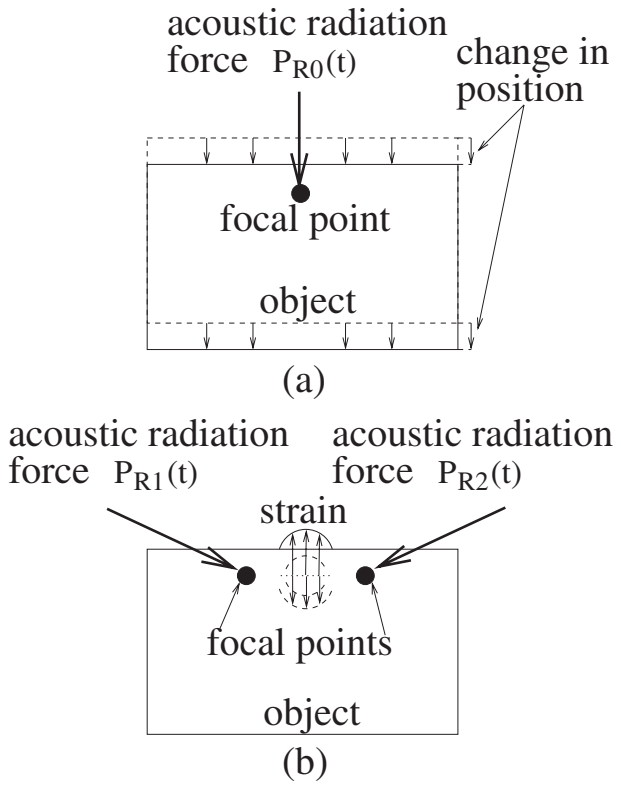

Fig. 1. Illustrations of (a) the change in position of an object caused by only one acoustic radiation force, and (b) the strain inside an object caused by two acoustic radiation forces.

acoustic radiation force per unit area of the interface as follows:[1,2)]

$$P_R(t) = (1 + R^2)e(t), \tag{2.1}$$

where R and $e(t)$ are the pressure reflection coefficient and the energy density at the interface, respectively. In eq. (2.1), the transmitted wave is assumed to be perfectly absorbed in the object. Using the densities, ρ_1 and ρ_2, and sound speeds, c_1 and c_2, of the medium and the object, the reflection coefficient, R, and the energy density, $e(t)$, are defined by

$$R = \frac{Z_2 - Z_1}{Z_2 + Z_1} = \frac{\rho_2 c_2 - \rho_1 c_1}{\rho_2 c_2 + \rho_1 c_1}, \tag{2.2}$$

$$e(t) = \frac{1}{\rho_1 c_1^2}\{p(t)\}^2, \tag{2.3}$$

where $p(t)$ is the sound pressure at the interface. The Japan Society of Ultrasonics in Medicine (JSUM) provides safety guidelines, in which the intensity of the CW ultrasound should be less than $1\,W/cm^2$. By assuming that the density ρ_1 and sound speed c_1 of water are $1.0 \times 10^3\,kg/m^3$ and 1,500 m/s, respectively, the acoustic radiation pressure, $P_R(t)$, exerted on the interface is calculated to be 6.67 Pa when the ultrasound intensity is $1\,W/cm^2$. In this calculation, the reflection coefficient, R, is assumed to be zero. For example, sound speeds of muscle and fat are 1,568 and 1,465 m/s, respectively.[34)] By assuming densities of these tissue to be $1.0 \times 10^3\,kg/m^3$, the reflection coefficient, R, is determined to be 0.034. Thus, the reflection coefficient can be assumed to be zero.

The energy density, $e(t)$, of the incident wave is proportional to the square of the sound pressure, $p(t)$, of the ultrasound beam. When two ultrasonic beams with slightly different frequencies, f and $f + \Delta f$, cross each other, the sound pressure, $p_{sum}(t)$, at the intersectional area is expressed by the sum of the sound pressures of two ultrasonic beams as follows:

$$p_{sum}(t) = p_0 \cos \omega t + p_0 \cos(\omega + \Delta\omega)t, \tag{2.4}$$

where p_0, ω, and $\Delta\omega$ are the amplitude of the sound pressure of each ultrasound beam, the angular frequency of the incident wave ($\omega = 2\pi f$), and the difference in angular frequency ($\Delta\omega = 2\pi\Delta f$), respectively. For this case, the energy density, $e(t)$, is given by

$$\begin{aligned} e(t) &= \frac{1}{\rho_1 c_1^2}\{p_{sum}(t)\}^2 \\ &= \frac{1}{\rho_1 c_1^2}\{p_0 \cos \omega t + p_0 \cos(\omega + \Delta\omega)t\}^2 \\ &= \frac{p_0^2}{\rho_1 c_1^2}\{1 + \cos \Delta\omega t + \cos(2\omega + \Delta\omega)t \\ &\quad + \frac{1}{2}\cos 2\omega t + \frac{1}{2}\cos 2(\omega + \Delta\omega)t\}. \end{aligned} \tag{2.5}$$

From the second term on the right-hand side of eq. (2.5), it is found that the energy density, $e(t)$, of the incident field has a component at the frequency difference Δf. Therefore, the cyclically oscillating radiation pressure, $P_R(t)$, at the frequency difference Δf is given by

$$P_R(t) = (1 + R^2)\frac{p_0^2}{\rho_1 c_1^2}(1 + \cos \Delta\omega t). \tag{2.6}$$

Thus, using an ultrasound beam generated by the sum of signals at slightly different frequencies, f and $f + \Delta f$, an oscillatory radiation force can be applied to the focal area of the beam.

In this study, in order to generate regional strain inside the object, we use two phase-controlled acoustic radiation pressures, $P_{R1}(t)$ and $P_{R2}(t)$, given by

$$P_{R1}(t) = (1 + R^2)\frac{p_{01}^2}{\rho_1 c_1^2}(1 + \cos \Delta\omega t), \tag{2.7}$$

$$P_{R2}(t) = (1 + R^2)\frac{p_{02}^2}{\rho_1 c_1^2}\{1 + \cos(\Delta\omega t + \Delta\phi)\}, \tag{2.8}$$

where $\Delta\phi$ is the phase difference between $P_{R1}(t)$ and $P_{R2}(t)$.

These two acoustic radiation forces at Δf, whose phase difference is $\Delta\phi$, are applied by setting focal points at two different sites inside the object. The insonification angles are assigned to θ_1 and θ_2 for respective transducers.

3. Experimental Setup

An experimental setup is illustrated in Fig. 2. In order to measure the strain, we employed ultrasonic diagnostic equipment (Toshiba SSH-160A) with a sector-type probe (center frequency: 5 MHz). The equipment was modified to detect the minute displacement of the object by the ultrasonic *phased tracking method*. An object made of gel ($45 \times 45 \times 17\,mm^3$, containing carbon powder to provide sufficient scattering) was placed in a water tank as shown in Fig. 2. For the application of radiation pressures, $P_{R1}(t)$ and $P_{R2}(t)$, two concave ultrasonic transducers were employed.

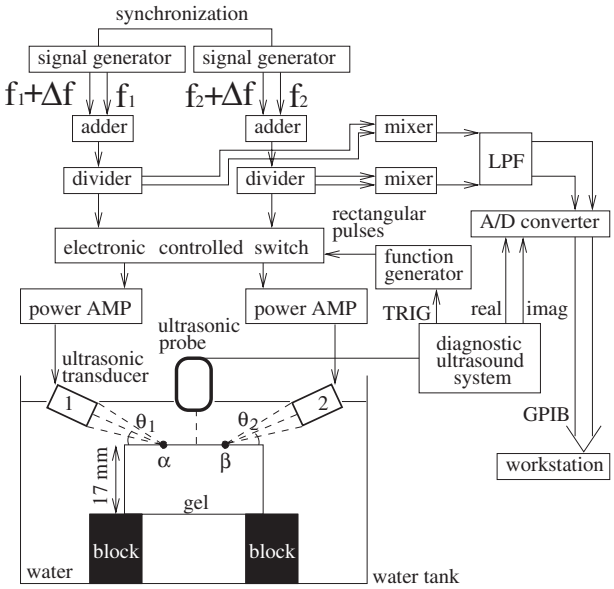

Fig. 2. Experimental setup for measurement of the strain inside an object cyclically actuated using two concave ultrasonic transducers.

A concave ultrasonic transducer (Tokimec 1Z20I-PF50-C; center frequency: 1 MHz) was driven by a sum of two CWs at two slightly different frequencies of 1 MHz and 1 MHz + 10 Hz. The resultant ultrasound beam was focused 50 mm away from the surface of the transducer, and the focal point was set at a point, α, on the top of the object with a beam angle, θ_1. Another concave transducer (Tokimec 1Z20I-PF50-C; center frequency: 1 MHz) was driven by the sum of CWs at 1 MHz and 1 MHz + 10 Hz. The focal point, which is 50 mm away from the surface of the transducer, was set at a point, β, on the top of the object with a beam angle, θ_2. The phase difference, $\Delta\phi$, between $P_{R1}(t)$ and $P_{R2}(t)$ was set to zero.

In this study, the spatial distributions of displacement (1) at the surface of the object and (2) inside the object are measured with a high speed video camera and ultrasound, respectively.

In the ultrasonic measurement, the CW ultrasound for actuation interferes with the pulsed ultrasound for the measurement of displacements. In order to avoid this interference, it is necessary to stop actuation during transmission and reception of the ultrasonic pulse for the measurement. Therefore, we used an electrical switch to control the cessation of the CW ultrasound for actuation.[10)]

4. Results

4.1 Displacement measurement with video camera

As illustrated in Fig. 3, four different sites, a, b, c, and d, at the surface on the side of the object were measured with a high speed video camera at a frame rate of 100 Hz. In this experiment, beam angles, θ_1 and θ_2, were set to 22 and 35°, respectively, and the distance between α and β was set to 6 mm. As shown in Fig. 3, focal areas of the two transducers were set at the edge of the top surface of the object. These four sites were measured for one cycle (100 ms) of acoustic radiation forces. Timing of the measured pictures relative to acoustic radiation forces is shown in Fig. 4. Bright spots in measured pictures correspond to the light reflected from

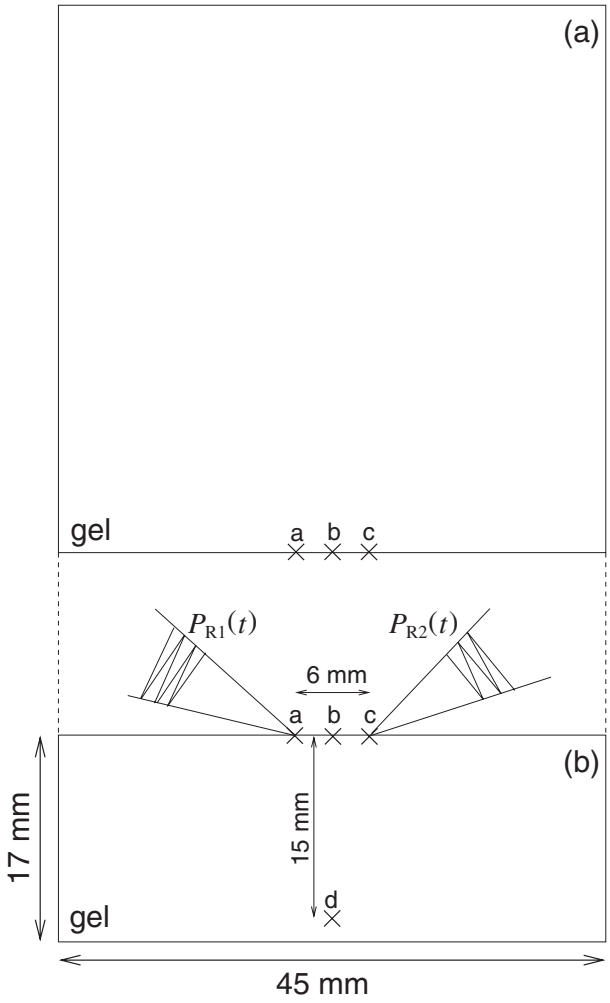

Fig. 3. Illustration of positions measured with a high-speed video camera. (a) Top view. (b) Side view.

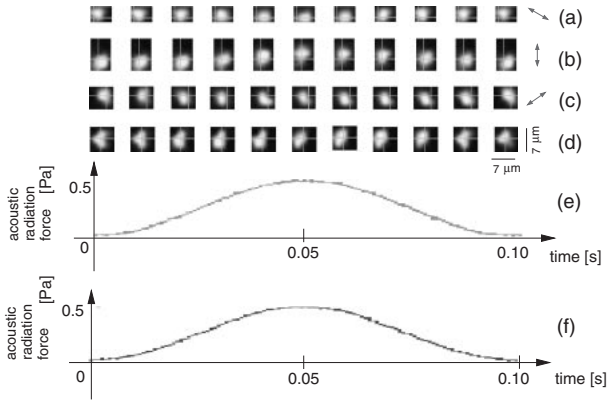

Fig. 4. Results obtained at point (a) a, (b) b, (c) c, and (d) d as indicated in Figs. 3. (e) and (f) Acoustic radiation forces radiated by two ultrasonic transducers.

carbon powder contained in the object due to the irradiation with the white light at a halogen lamp. At points a and c (two focal points), displacements in the directions of respective ultrasonic beams were obtained as shown in Figs. 4(a) and 4(c). As shown in Fig. 4(b), point b moved upward when acoustic radiation forces increased. This result shows that the region between two focal points was vertically thickened

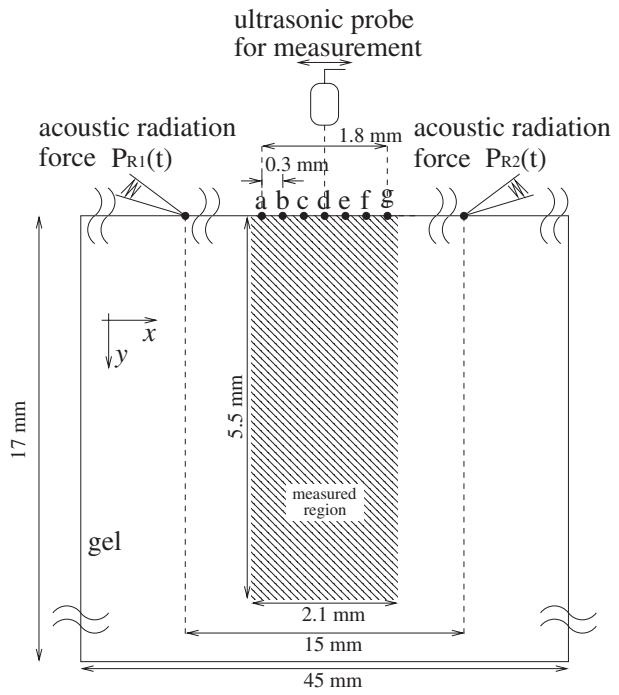

Fig. 5. Illustration of positions measured with ultrasound.

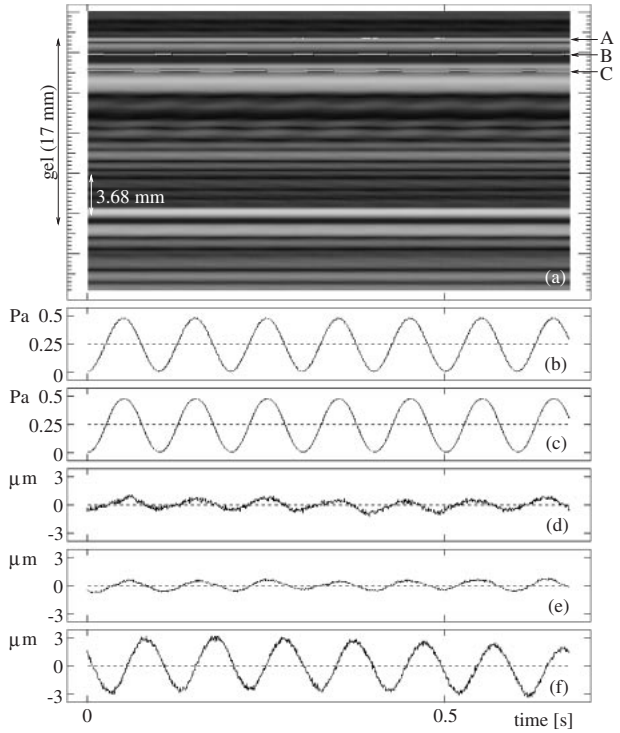

Fig. 6. (a) M-mode image of an object. (b) Acoustic radiation pressure, $P_{R1}(t)$. (c) Acoustic radiation pressure, $P_{R2}(t)$. (d) Displacement at point A (surface) indicated in (a). (e) Displacement at point B (1.5 mm from the surface). (f) Displacement at point C (3.0 mm from the surface).

due to horizontal compression by application of dual acoustic radiation force.

4.2 Displacement measurement with ultrasound

The spatial distribution of displacements inside the object was measured with ultrasound. In this experiment, angles θ_1 and θ_2 of both beams were set to 25°, and the distance between α and β was set to 15 mm. The positions measured are illustrated in Fig. 5. Figure 6(a) shows an M-mode image of the object obtained at measured position d. Acoustic radiation pressures, $P_{R1}(t)$ and $P_{R2}(t)$, shown in Figs. 6(b) and 6(c) were calculated based on eq. (2.6) as follows: The density, ρ_2, and the sound speed, c_2, of the object were measured as $1.1 \times 10^3\,\mathrm{kg/m^3}$ and 1.47×10^3 m/s, respectively. By assuming the density, ρ_1, and the sound speed, c_1, of water to be $1.0 \times 10^3\,\mathrm{kg/m^3}$ and 1.5×10^3 m/s, respectively, the pressure reflection coefficient, R, and the energy reflection coefficient, R^2, respectively were calculated as 0.038 and 0.0014 using eq. (2.2). Therefore, in this study, by assuming the object to be a totally absorbent material ($R = 0$), the acoustic radiation pressures, $P_{R1}(t)$ and $P_{R2}(t)$, exerted on two points, α and β, in the object were calculated based on eq. (2.6). In this calculation, we obtained the amplitude of the focused sound pressures of p_{01} and p_{02} beforehand by measuring the acoustic fields of each ultrasound for actuation with a hydrophone (Force Institute, MH-28-10).

In Fig. 6(d), the displacement, $d(t)$, at the surface (point A) of the object actuated by the acoustic radiation forces was measured by the ultrasonic *phased tracking method*. Tracking lines were superimposed with gray lines on the M-mode image in Fig. 6(a). In Fig. 6(d), it is found that the object was cyclically actuated with an amplitude of a few micrometers,[10] which was similar to that measured with the high speed video camera.

Two acoustic radiation forces were applied by setting focal points at the upper surface of the object, and angles θ_1 and θ_2 of both ultrasonic beams for actuation were set to 25°. Therefore, directions of horizontal components of these two acoustic radiation forces opposed each other by setting $\Delta\phi = 0$. Therefore, the region between the two focal points was cyclically compressed along the horizontal axis by these acoustic radiation forces, and the thickness of the region between two focal points increases along the vertical axis.

Figures 6(d)–6(f) show displacements at multiple points along an ultrasonic beam. When the acoustic radiation forces shown in Figs. 6(b) and 6(c) increase, the surface of the object and a point which was 1.5 mm deeper than the surface moved upward [Figs. 6(d) and 6(e)]. On the other hand, a point which was 3.0 mm deeper than the surface moved downward as shown in Fig. 6(f). This result shows that the thickness of the region between two focal points increased along the vertical axis, which shows that strain was generated inside the object.

The two-dimensional displacement distribution was measured by moving the ultrasonic probe for the measurement in the horizontal direction as illustrated in Fig. 5. The displacement, $d(t)$, at every sampled point along each ultrasonic beam was obtained, and the amplitude of the displacement, $d(t)$, at the frequency difference, $\Delta f = 10$ Hz, was estimated by applying the Fourier transform to the displacement, $d(t)$, and the acoustic radiation pressure, $P_{R1}(t)$, with a Hanning window of 0.68 s (1024 points). In addition, the phase delay of the displacement, $d(t)$, from the acoustic radiation pressure, $P_{R1}(t)$, was also estimated. In Fig. 7, phase delays of displacements, $d(t)$, were color-coded. Amplitudes of displacements, $d(t)$, were indicated by the brightness of the

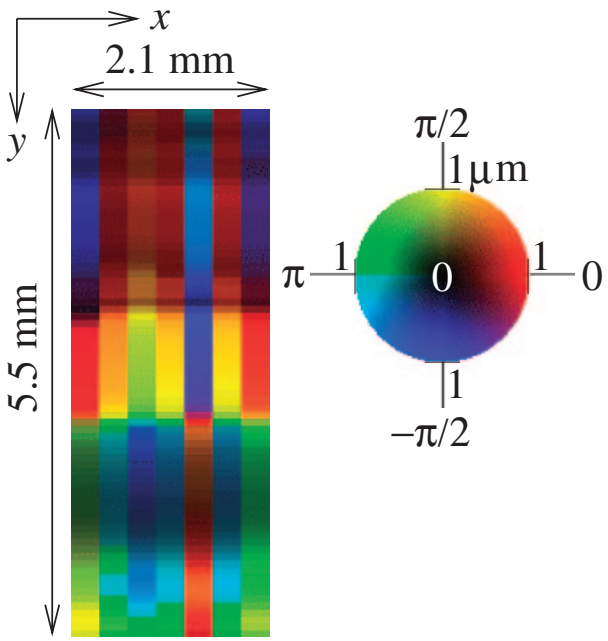

Fig. 7. Spatial distribution of displacements inside an object.

color. A phase difference of zero shows that that point moves upward when the acoustic radiation force increases. In Fig. 7, the region near the top surface tends to move upward when the radiation force increases. On the other hand, the region which is 3.0 mm deeper than the top surface tends to move downward. From these results, it was found that strain inside the object was successfully generated using two phase-controlled acoustic radiation forces.

5. Discussion

In this study, the spatial distribution of displacements caused by two acoustic radiation force was measured with ultrasonic *phased tracking method*. The applied acoustic radiation forces and resulting displacement distribution are discussed in the following. Figure 8(a) shows the sound pressure distribution generated by the ultrasonic transducer used for actuation. From Fig. 8(a), it was assumed that the width at half maximum of the acoustic radiation force is about 5 mm along the x-axis, and the acoustic radiation force was almost constant along the z-axis in the object. Therefore, the region in which the acoustic radiation force was over the half maximum is roughly considered as shown by the shadowed region in Fig. 8(b). In Fig. 8(b), the measured region is surrounded by a dashed line. Two ultrasound beams crossed each other at a depth of about 4 mm from the top surface. At each point in the region within 4 mm of the top surface in the measured region, the sum of horizontal components caused by two acoustic radiation pressures, $P_{R1}(t)$ and $P_{R2}(t)$, is not zero (Magnitudes of these components are different.). Therefore, the region within 4 mm of the top surface was compressed along the horizontal axis, and, as shown in Fig. 7, the resulting upward displacement during the increase in acoustic radiation forces was found.

Around 4 mm from the top surface, horizontal components of two acoustic radiation forces almost compensated for each other, and only vertical components remained.

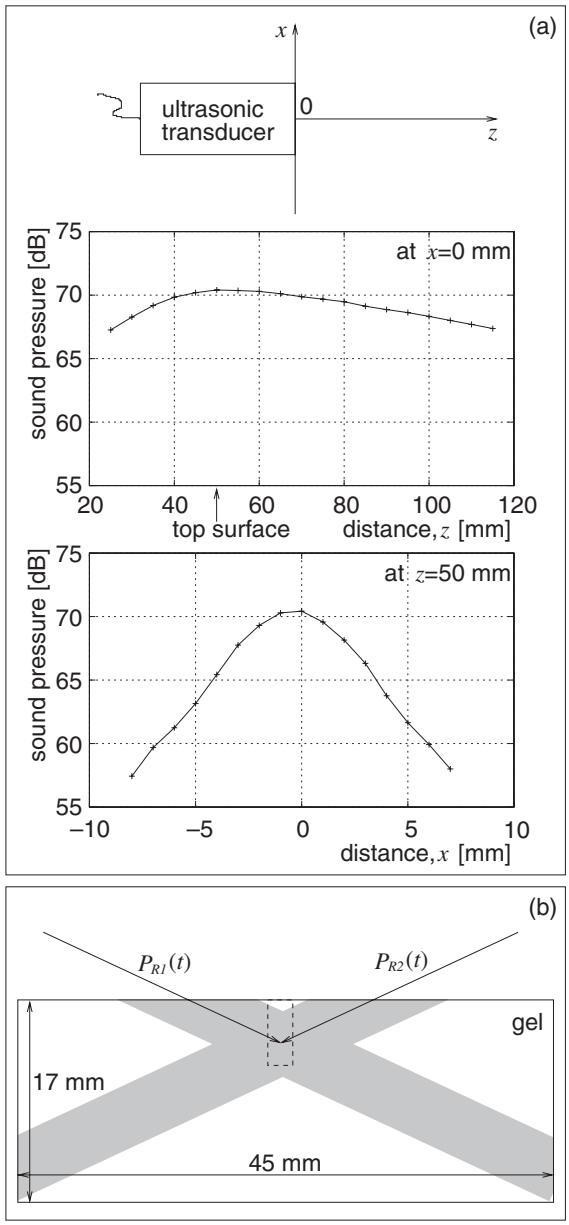

Fig. 8. (a) Sound field generated by the ultrasonic transducer used for actuation. (b) Consideration of displacement distribution generated by two acoustic radiation forces.

Therefore, the region around 4 mm from the top surface moves downward during the increase in acoustic radiation force because of the downward displacement caused by vertical components of acoustic radiation forces as well as that caused by the horizontal compression in the region nearer than 4 mm from the top surface.

As shown in Fig. 7, the measured displacement distribution showed that strain inside the object was successfully generated. However, at this moment, it is difficult to estimate the elastic modulus distribution precisely because of the problems described below.

- Measurement of strain distribution
  The stress applied by the acoustic radiation force is not plane stress. Therefore, the region where the acoustic radiation force is applied is displaced in not only one direction. However, in this study, only the beam-axis component of displacement was measured. To obtain

precise strain and elastic modulus distributions, a method for measuring three dimensional components of displacement is needed.

- Estimation of magnitude of applied stress
  Equation (2.6) used for estimation of the magnitude of the acoustic radiation force was derived by assuming the object to be a perfectly absorbing material. However, the attenuation coefficient of soft tissue has a finite value. For example, the attenuation coefficient of the mixture of muscle and fat (abdominal wall) is typically $3\,\mathrm{dB\cdot cm^{-1}\cdot MHz^{-1}}$.[34] To estimate the magnitude of the applied acoustic radiation force, the attenuation coefficient of tissue must be considered.
- Estimation of stress distribution
  Figure 8(a) shows the sound pressure distribution, which is directly related to the acoustic radiation force as shown by eq. (2.6), generated by the ultrasonic transducer used for application of the acoustic radiation force. As shown in Fig. 8(a), the acoustic radiation force is a function of the geometry, and the stress distribution must be considered in addition to the strain distribution.

Furthermore, the distance between two focal points, beam angles, and the depth of the region of interest is restricted by the factors described in the following.

When focal areas of two ultrasonic transducers overlap, the horizontal components of the two acoustic radiation forces compensate for each other in the intersectional area. Therefore, for effective generation of strain, two focal points are assigned so that sound fields generated by the two transducers do not overlap within the object (= region of interest). On the other hand, when the distance between two focal points is very large in comparison with the size of the focal area, the displacement distribution is not so different from that caused by one acoustic radiation force. Therefore, the size of the region of interest (between two focal areas) should be comparable to the width of the ultrasonic beam.

Furthermore, to keep the beam angles θ_1 and θ_2 similar at every depth, the distance between two focal points should be changed in relation to the depth of the region of interest. This is done using a phased array probe.

As described above, it is currently difficult to estimate the "absolute" elastic modulus precisely using the proposed method. Therefore, the elasticities of different individuals measured by the proposed method are difficult to compare. However, for example, the temporal change or frequency dependence of the strain distribution within an individual is directly related to the change in elastic properties. The proposed method can detect such a relative change in the elastic property of an object.

6. Conclusions

In this study, in order to generate regional strain inside an object, we constructed an experimental setup for the application of cyclic remote actuation in an object using two focused ultrasonic transducers. The phase difference between the two acoustic radiation forces, which were applied at two different positions in the object, was controlled to 0°. The resultant displacements inside the object were successfully measured by the ultrasonic *phased tracking method*. These results show the potential of the proposed method for the generation of regional strain inside an object.

1) M. Fatemi, L. E. Wold, A. Alizod and J. F. Greenleaf: IEEE Trans. Med. Imaging **21** (2002) 1.
2) M. Fatemi and J. F. Greenleaf: Proc. Natl. Acad. Sci. U.S.A. **96** (1999) 6603.
3) G. R. Torr: Am. J. Phys. **52** (1984) 402.
4) K. Nightingale, M. S. Soo, R. Nightingale and G. Trahey: Ultrasound Med. Biol. **28** (2002) 227.
5) G. E. Trahey, M. L. Palmeri, R. C. Bentley and K. R. Nightingale: Ultrasound Med. Biol. **30** (2004) 1163.
6) B. J. Fahey, K. R. Nightingale, R. C. Nelson, M. L. Palmeri and G. E. Trahey: Ultrasound Med. Biol. **31** (2005) 1185.
7) Japan Society of Ultrasonics in Medicine: Cho-onpa Igaku **11** (1984) 41 [in Japanese].
8) H. Kanai, M. Sato, Y. Koiwa and N. Chubachi: IEEE Trans. Ultrason. Ferroelectr. Freq. Control **43** (1996) 791.
9) H. Kanai, H. Hasegawa, N. Chubachi, Y. Koiwa and M. Tanaka: IEEE Trans. Ultrason. Ferroelectr. Freq. Control **44** (1997) 752.
10) K. Michishita, H. Hasegawa and H. Kanai: Jpn. J. Appl. Phys. **42** (2003) 4608.
11) H. Kanai, K. Sugimura, Y. Koiwa and Y. Tsukahara: Electron. Lett. **35** (1999) 949.
12) M. Watanabe and H. Kanai: Jpn. J. Appl. Phys. **40** (2001) 3918.
13) M. Watanabe, H. Hasegawa and H. Kanai: Jpn. J. Appl. Phys. **41** (2002) 3613.
14) H. Hasegawa and H. Kanai: IEEE Trans. Ultrason. Ferroelectr. Freq. Control **53** (2006) 52.
15) H. Hasegawa, H. Kanai, N. Hoshimiya and Y. Koiwa: Jpn. J. Appl. Phys. **39** (2000) 3257.
16) H. Hasegawa, H. Kanai and Y. Koiwa: Jpn. J. Appl. Phys. **41** (2002) 3563.
17) H. Kanai, Y. Koiwa and J. Zhang: IEEE Trans. Ultrason. Ferroelectr. Freq. Control **46** (1999) 1229.
18) H. Kanai, H. Hasegawa, M. Ichiki, F. Tezuka and Y. Koiwa: Circulation **107** (2003) 3018.
19) H. Hasegawa, H. Kanai, Y. Koiwa and J. P. Butler: Jpn. J. Appl. Phys. **42** (2003) 3255.
20) H. Hasegawa, H. Kanai and Y. Koiwa: IEEE Trans. Ultrason. Ferroelectr. Freq. Control **51** (2004) 93.
21) H. Hasegawa and H. Kanai: Jpn. J. Appl. Phys. **43** (2004) 3197.
22) N. Nakagawa, H. Hasegawa and H. Kanai: Jpn. J. Appl. Phys. **43** (2004) 3220.
23) J. Tang, H. Hasegawa and H. Kanai: Jpn. J. Appl. Phys. **44** (2005) 4588.
24) J. Inagaki, H. Hasegawa, H. Kanai, M. Ichiki and F. Tezuka: Jpn. J. Appl. Phys. **44** (2005) 4593.
25) H. Hasegawa and H. Kanai: Jpn. J. Appl. Phys. **44** (2005) 4609.
26) M. Sugimoto, H. Hasegawa and H. Kanai: Jpn. J. Appl. Phys. **44** (2005) 6297.
27) H. Kanai, S. Nakaya, H. Honda and Y. Koiwa: Electron. Lett. **35** (1999) 765.
28) H. Kanai, Y. Koiwa, Y. Saito, I. Susukida and M. Tanaka: Jpn. J. Appl. Phys. **38** (1999) 3403.
29) H. Kanai, S. Yonechi, I. Susukida, Y. Koiwa, H. Kamada and M. Tanaka: Ultrasonics **38** (2000) 405.
30) H. Kanai and Y. Koiwa: Ultrasound Med. Biol. **27** (2001) 481.
31) Y. Koiwa, H. Kanai, H. Hasegawa, Y. Saitoh and K. Shirato: Ultrasound Med. Biol. **28** (2002) 1395.
32) H. Kanai, Y. Koiwa, S. Katsumata, N. Izumi and M. Tanaka: Jpn. J. Appl. Phys. **42** (2003) 3239.
33) H. Kanai: IEEE Trans. Ultrason. Ferroelectr. Freq. Control **51** (2005) 1931.
34) S. A. Goss, R. L. Johnston and F. Dunn: J. Acoust. Soc. Am. **64** (1978) 423.